CHAPTER

II.5

NANOSCALE THERMOPHYSICAL PHENOMENA FROM MOLECULAR DYNAMICS SIMULATION: RECENT ADVANCES

Jennifer R. Lukes, Alexis R. Abramson, and Jian-Gang Weng

Abstract

Molecular dynamics simulation is an increasingly popular technique for investigating the fundamental thermophysical processes that occur at small length and time scales. This article reviews recent molecular dynamics studies on thermal transport in nanostructures and molecules, short time-scale laser-material interactions, and liquid-vapor interfacial phenomena, and summarizes the various computational methodologies applied in these studies. Key directions for future research in these areas include clarification of physical mechanisms responsible for the unique thermal transport in nanostructures, incorporation of simplified quantum-mechanical techniques in the modeling of laser-material interactions, investigation of surface tension behavior in multicomponent fluids, and unambiguous determination of the Tolman length for curved interfaces.

1-56700-222-6/04/$35.00+$00.00

1 INTRODUCTION

1.1 Need for Atomic-Scale Modeling

Many of today's materials, devices, and processes are approaching fundamental length and time scales below which certain macroscopic assumptions break down. For example, semiconductor superlattice structures in quantum-well lasers, due to their nanometer-scale characteristic dimensions and the dominant effect of interfaces, exhibit unusual electronic and thermal properties that cannot be predicted from conventional averaging of the properties of the constituent layers. Also, ultrashort-pulse laser material interaction studies reveal novel ablation phenomena related to the nonthermal processes occurring at femtosecond time scales. A better fundamental understanding of the physical phenomena occurring at small length and time scales is needed in order to design and analyze new devices and processes. Unfortunately, continuum phenomenological models are questionable in such regimes and theoretical analysis of these effects is often intractable for all but the simplest systems. Numerical simulation of the individual particles in a system, on the other hand, is a useful tool for capturing atomic-scale events and phenomena that affect the behavior of the system. Computational modeling in this regard provides analysis of the effects of extreme conditions and very short length and time scale phenomena that can be difficult to assess with experiments.

1.2 Quantum Material Modeling

Subcontinuum material modeling can be performed at varying levels of complexity, ranging from classical to fully first principles simulation. In cases where bond breaking, polarization, and electronic structure are important, sophisticated approaches based on quantum mechanics are required [1]. There are two primary classifications of quantum-mechanical methods: first principles (ab initio) and semiempirical.

1.2.1 Ab Initio Methods. Ab initio methods, the most fundamental quantum-mechanical modeling methods, are derived solely from the positions and atomic numbers of each atom in the system and require no adjustable parameters. They give the most accurate results of any simulation technique, but are extremely involved and can currently treat only on the order of 100 atoms. The most prominent ab initio methods are Hartree-Fock [2–4], which is most useful for quantum chemical studies of individual molecules, and density functional theory [5, 6], which has achieved wide success in solid-state physics [7]. The Hartree-Fock method expresses the total system energy in terms of the wave function of each electron, while density functional theory expresses it more simply in terms of the ground-state electron density of the system. Of the various techniques used to combine density functional theory and molecular dynamics, Car-Parrinello molecular dynamics [8] is the most widely used.

1.2.2 Semiempirical Methods. Semiempirical quantum-mechanical methods significantly reduce computational complexity by incorporating into the computations empirical parameters from experiments or ab initio studies. These methods are less accurate and less general than the full ab initio method, but can treat much larger systems while still retaining important quantum-mechanical features. Two widely used semiempirical approaches include the modified neglect of diatomic overlap (MNDO) method [9] and the tight-binding method [10]. The MNDO and subsequent related methods are primarily employed in studies of small organic molecules, while tight-binding methods are most useful for inorganic condensed matter, such as covalent and transition metal systems. For more detail on the above quantum simulation methods, the reader may find a good introduction in [7, 11].

1.3 Classical Material Modeling and Methods

Although much less involved than full ab initio methods, semiempirical methods are still intractable for systems larger than a few nanometers. Classical atomistic simulations are computationally much less expensive, and provide a convenient means for analyzing material behavior at these length scales in cases where electronic effects are not important. Such simulations are useful for modeling a wide variety of physical phenomena including solid-vapor-liquid interfaces and atomic-scale friction [12, 13]. Classical simulation treats atoms as classical particles and calculates material properties based on the motions of these atoms. Key classical modeling techniques include molecular mechanics [14], which minimizes system energy to find the most stable structure; lattice dynamics [15], which yields dispersion relations given an intermolecular potential; Monte Carlo, first used by Metropolis and Ulam [16] and described in detail by Binder [17], which determines particle positions stochastically by analyzing randomly chosen movements and the associated potential energies of the new configurations; and molecular dynamics [18–20], which deterministically models the trajectories of particles that interact according to a force field or empirical potential using the classical equations of motion.

1.3.1 Molecular Dynamics Simulation. Molecular dynamics simulation (MD) is widely used by chemists, physicists, biologists, and engineers to examine structure, behavior, and mechanical and physical properties in a wide range of molecular and atomic systems. The primary advantage of this technique over the other classical techniques introduced above is that it can capture dynamical and transport processes in a physically meaningful way. The only parameters required in MD are initial positions and velocities of each atom in the system and an interatomic potential energy function. This function describes the attractive and repulsive interactions between atoms due to the nature of their overlapping electron clouds. Forces on atoms are calculated by taking the negative of the derivative of the interatomic potential with respect to position. The total force on a particular atom is determined by summing up its force interactions with all the other atoms in the system. For potentials

where long-range interactions are very small, the force calculation can be simplified considerably by neglecting faraway atoms beyond a certain "cutoff" distance. Given these forces and the initial positions and velocities, the atoms are marched forward in time. The resultant atomic trajectories can be analyzed and the data used to provide insight into microscopic and short-time-scale processes as well as to calculate physical properties of interest, such as thermal conductivity, atomic-structure factor, and surface tension. The main limitations of MD are that the results depend on the availability of a suitable intermolecular potential and that it is limited to small length and time scales. Nanoscale systems and processes whose characteristic time scales are on the order of nanoseconds and shorter are thus well suited to study by MD, but bulk systems can also be treated with an appropriate application of periodic boundary conditions.

1.3.2 Common Intermolecular Potentials. In general, the potential experienced by an atom may be divided into terms to include the energy on the atom itself due to an external field and the energy due to atomic interactions. The interatomic interactions may depend on contact between pairs, triplets, quadruplets, and higher combinations of atoms and therefore can be quite complicated. The particular form of the intermolecular potential depends on the nature of the bonding of a material. Potentials commonly applied to covalently bonded materials include the Stillinger-Weber potential for silicon [21] and the Tersoff-Brenner potential [22], which has been used extensively to model carbon and hydrocarbon systems. Metallic systems are typically handled using the embedded atom model [23] or the Finnis-Sinclair model [24]. Liquid water is widely treated using intermolecular potentials based on the single point charge (SPC) [25] or transferable intermolecular potential (TIP) [26] models. The classical, widely used Lennard–Jones (LJ) model

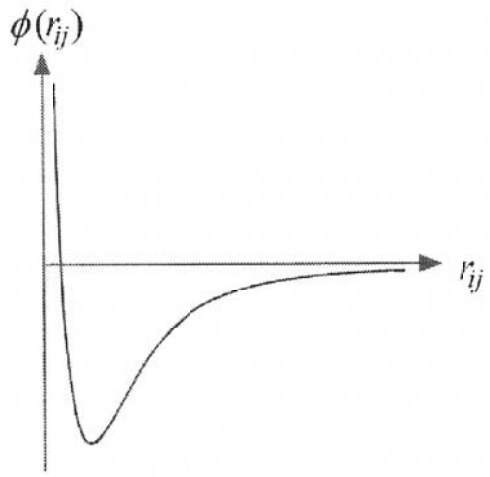

Figure 1 Lennard–Jones intermolecular potential model.

(Figure 1), which describes well the potential energy interactions ϕ_{ij} between filled-valence shell inert elements as a function of interatomic separation r_{ij}, provides a convenient means to gain qualitative insight into the fundamental physics governing a broad range of material systems.

1.4 Scope

Molecular dynamics simulation is a broad and active field. The review presented herein focuses on MD studies that contribute to the fundamental understanding of thermophysical phenomena at small length and time scales. In particular, thermal transport in nanostructures and molecules, short-time-scale laser-material interactions, and liquid-vapor interfacial phenomena are treated. Works from the last five years and those not reviewed in other articles are covered. For further background on MD simulation and its application to microscale and nanoscale thermophysical engineering, the interested reader is referred to earlier works in the literature [1, 12, 13, 18–20, 27, 28].

2 THERMAL TRANSPORT IN NANOSTRUCTURES AND MOLECULES

2.1 Thermal Conductivity and Temperature Calculation

Although MD cannot accurately capture electronic transport without invoking complex ab initio calculations, vibrational energy transport is relatively easy to examine and analyses of lattice thermal conductivity are commonly performed. The Green–Kubo method [29] is a popular thermal conductivity calculation technique based on equilibrium simulations of the heat flux autocorrelation function over a sufficiently long time period. Another technique is the homogeneous nonequilibrium technique [30, 31], in which artificial forces are added to the equations of motion to represent the effect of an external thermal field without the presence of a temperature gradient. A third technique is to impose a temperature gradient or, alternatively, a heat flux across the system of interest (Figure 2). Using the Fourier law, the heat flux and temperature gradient across the "regular" atoms are used to calculate thermal conductivity. Regardless of the particular technique used, the temperature or local temperature of the system must be known. As long as local thermodynamic equilibrium exists, or in other words if the local velocity distribution is Maxwellian, a local temperature can be calculated from the squares of the velocities of the atoms in the region. The steady-state temperature may be described by an average over an appropriately chosen ensemble of atoms, or equivalently over an adequate time period as is carried out for these MD simulations.

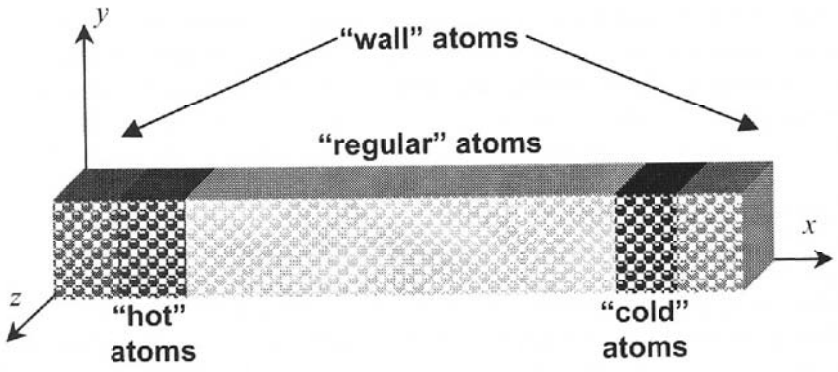

Figure 2 Schematic of simulation cell for nonequilibrium thermal conductivity calculation.

2.2 Dynamic Structure Factor Calculation

Molecular dynamics simulations provide information about time-dependent quantities that fluctuate about a mean value. These random fluctuations occur due to the continuously changing interactions among atoms and redistribution of energies. Recording and studying the fluctuations reported via MD simulations allows other important sources of information about the system to be collected. One such parameter of interest is the dynamic structure factor, which provides an examination of the nature of the distribution of atoms as a function of time. In terms of probability, the dynamic structure factor measures the probability that at time $t + dt$, an atom is at a particular distance (or wave vector) from an equilibrium value, given that the same atom was at the equilibrium value at time t. In reciprocal space, the dynamic structure factor $S(\boldsymbol{q}, t)$ may be evaluated by the following relation [18]

$$S(q,t) = \frac{1}{\tau_{\max}} \sum_{\tau_0}^{\tau_{\max}} \rho(q, t_0 + dt)\rho(-q, t_0) \tag{1}$$

and ρ, the density distribution function, can be determined by

$$\rho(q,t) = \sum_j \exp[-i\boldsymbol{q} \cdot \boldsymbol{r}_j(t)], \tag{2}$$

where the sum is over the group of atoms of interest and $\tau_{\max}$ is the maximum time over which the correlation is made. This is essentially the spatial Fourier transform of the number density. This requires that the position of each atom be recorded as a function of time throughout the simulation, thereby capturing the fluctuations in position of the system. In a simulation with periodic boundary conditions, there are only a set number of allowed wave vectors for which the dynamic structure factor can be calculated such that

$$\boldsymbol{q} = \frac{2\pi}{a}\left(\frac{n_x}{N_x}\boldsymbol{b}_1 + \frac{n_y}{N_y}\boldsymbol{b}_2 + \frac{n_z}{N_z}\boldsymbol{b}_3\right), \tag{3}$$

where $\boldsymbol{b}_1$, $\boldsymbol{b}_2$, and $\boldsymbol{b}_3$ are the unit vectors in reciprocal space, and n_x, n_y, and n_z are integer values from 1 to N_x, N_y, and N_z, which correspond to the number of atoms in each of the respective directions. Performing a Fourier transform of the dynamic structure factor from time to frequency space gives $S(\boldsymbol{q}, \omega)$. This parameter may be measured experimentally by inelastic neutron scattering. A plot of the power spectrum of the dynamic structure factor $|S(\boldsymbol{q}, \omega)|^2$ for any allowed value of $\boldsymbol{q}$ should demonstrate peaks that correspond to an allowed frequency at that particular wave vector. In other words, this plot provides information about the dispersion relation of the atomic system studied via MD simulations. Information regarding the dispersion relation is useful as an input for Monte Carlo simulations. Moreover, it provides insight into the nature of the atomic vibrations, and therefore may be used to help assess the impact of mechanisms such as miniband formation on thermal energy transport.

2.3 Individual Structures and Molecules

Thermal transport in materials with microscale or nanoscale characteristic dimensions deviates from that in bulk materials. For example, the thermal conductivity in molecules, such as carbon nanotubes, is significantly higher than in bulk carbon, while in nanostructures, such as thin films, superlattices, and nanowires, it is much lower than the corresponding bulk thermal conductivity. While there has been much research on nanoscale size effects in the past two decades, the particular physical mechanisms affecting thermal transport and the conditions under which they become important are the subject of ongoing debate. A variety of mechanisms, such as acoustic impedance and phonon spectra mismatch, miniband formation, and a corresponding phonon group velocity reduction, phonon tunneling, and interface scattering due to roughness, defects, or dislocations, have been proposed as contributors to the observed deviations. Lattice strain, commonly exhibited by symmetrically and asymmetrically strained superlattices, may also play a significant role in affecting thermal transport. Employing MD simulations to investigate thermal transport in nanostructures may provide insight into the significance and complexity of these mechanisms.

2.3.1 Thin Lennard–Jones Films. Two recent papers have investigated thermal conduction in nanometer-scale LJ argon thin films. Lukes et al. [32] investigated thermal conduction size effects in three-dimensional thin films. In agreement with observed data and theoretical predictions, the results show that thermal conductivity increases with film thickness and that thermal conduction size effects are more pronounced at low temperatures. The calculated values are high by about 30%, which is reasonable given the fact that the only assumptions used in the calculations were the LJ intermolecular potential and constant thermal conductivity. The authors also enumerate practical guidelines for ensuring efficient steady-state simulations, including running data generation simulations for at least twenty times the estimated

thermal diffusion time of the material, increasing simulation time rather than particle number where feasible, and performing high-temperature simulations where possible. Xue and Shu [33], in their study of the time-dependent thermal transport in a two-dimensional LJ film, used a different metric to quantify when the system has reached a stationary state. To ensure that the simulation has sampled a representative region of phase space, they monitor both the instantaneous Boltzmann H function and the translational order parameter of Verlet [34] for all the atoms in the system. These two parameters are single numbers that are related to the maximization of entropy and to randomization of atomic position, respectively, and it is easier to track their temporal evolution than that of the distribution of particle velocities. Although it may be more appropriate to monitor the H function in regions of local thermodynamic equilibrium rather than over the whole system, the authors find an asymptotic approach to the value predicted from the Maxwell distribution and also find qualitative agreement with the order parameter behavior. Additionally, they find that steady state is approached much more quickly with the introduction of interfaces and void defects.

2.3.2 Silicon Nanowires. As a consequence of boundary scattering in one-dimensional nanowires, the thermal conductivity may be reduced beyond what might be expected in a thin film of similar material. Furthermore, other important phonon transport mechanisms may be responsible for influencing heat flow. While there have been a number of recent studies on thermal transport in nanowires, few of those investigations have utilized molecular dynamics techniques. Volz and Chen [35] first performed MD simulations to determine the thermal conductivity of square silicon nanowires. They employed the Stillinger–Weber interatomic potential and the Green–Kubo formulation to find a reduction of one to two orders of magnitude compared to bulk silicon. Their data are in good agreement with a standard Boltzmann transport equation (BTE) solution when a specularity parameter of 0.45 is used. Lu et al. [36, 37] used the equation of phonon radiative transfer (EPRT) with temperature and frequency dependent relaxation times to explain the MD results of Volz and Chen and demonstrated that the EPRT and MD data are in good agreement when a boundary specularity parameter of 0.35 was assumed. The authors suggest that the 0.35 value is more reasonable than the BTE value of 0.45 because more detailed relaxation time information was included in its determination. While insight into nanoscale thermal transport was provided by these investigations, no conclusive evidence was given to clearly explain the mechanisms responsible for the reduction in thermal conductivity.

2.3.3 Carbon Nanotubes. Molecular dynamics simulations of carbon nanotubes (CNTs) have been used extensively over the past few years to explore the unique behavior of these nanoscale molecules. To investigate the thermal properties of CNTs, the Tersoff–Brenner interatomic potential [38] is often employed in classical MD simulations, and the electronic contribution to thermal conductivity

is assumed negligible due to the low density of free carriers [39]. In 2000, Osman and Srivastava [40] demonstrated a peaking behavior of thermal conductivity of carbon nanotubes as a function of temperature using a nonequilibrium MD simulation with periodic boundary conditions. In contrast to recent experimental data on silicon nanowires [41], in which peak temperature increased with decreasing diameter, the peak temperatures from the simulations decreased with decreasing diameter. No dependence of peak position on chirality was observed. The explanation Osman and Srivastava offer for the shift is that smaller diameter nanotubes have larger minimum wave vectors, leading to more likelihood of wave vectors that exceed the Brillouin zone boundary and thus resulting in an earlier (lower-temperature) onset of Umklapp scattering. The authors also indicate that radial phonons provide the primary contribution to thermal transport in the nanotubes. Berber et al. [42] used homogeneous nonequilibrium molecular dynamics simulations [31,43] to determine the thermal conductivity of CNTs as a function of temperature. They demonstrated an unusually high maximum value of 6600 $W/m \cdot K$ at room temperature, which they attribute to very long phonon mean free paths. Like Osman and Srivastava, they also found a peak in temperature-dependent thermal conductivity. Results for a similar (10, 10) nanotube using a simple nonequilibrium MD simulation from Osman and Srivastava [40], however, give a value of approximately 1500 $W/m \cdot K$. One possible reason for this disparity is the difference in nonequilibrium simulation techniques applied: nonhomogeneous nonequilibrium MD [40] versus homogeneous nonequilibrium MD [42]. Another reason for the lower value found by Osman and Srivastava may be the finite size effect that results from the mean free path limitations on phonons created by defining the simulation cell between hot and cold baths. Maruyama [44] explored the finite size effect in CNTs by utilizing a nonhomogeneous nonequilibrium MD simulation along with free boundary conditions and applying a phantom heat-bath model to both ends of the single-wall CNT. His results demonstrate a general increase in thermal conductivity with CNT length from approximately 10 – 100 nm, but exhibit values an order of magnitude lower than Osman and Srivastava, who applied the same technique to tubes of comparable length using periodic boundary conditions. This discrepancy may be caused by the difference in boundary conditions used in the two simulations. Che et al. [45] were the only group to perform equilibrium MD calculations on CNTs, reporting a converged room temperature thermal conductivity of 2980 $W/m \cdot K$.

2.3.4 Solid-Solid Interfacial Regions. Molecular dynamics is particularly suitable for investigating interfacial regions, and the application of this technique to systems where interfaces strongly affect thermal transport has become more widespread over the past few years. In 2000, Liang and Shi [46] carried out two-dimensional MD simulations to examine the effect of atomic mass and interatomic potential parameters on the thermal conductivity of Lennard–Jones superlattices. Volz et al. [47,48] applied novel MD techniques to model a Si/Ge superlattice system and found that the thermal conductivity results for layer thicknesses of 23 and 33 Å corresponded well to experimental data. In 2002, Abramson et al. [49] per-

formed MD simulations to determine the effective thermal conductivity of simple Lennard–Jones heterostructures by varying key parameters, such as film thickness, numbers of interfaces per unit length, and interfacial strain. Of particular value was their insight into the critical contribution of interfacial strain to interfacial thermal conductance. Similar studies to investigate the role of strain on heat transport in nanostructures were also conducted by Picu et al. [50] and Yang et al. [51]. Twu and Ho [52] utilized MD to examine conductance across the interface formed by two dielectric thin films. They found that low temperatures lead to a large temperature jump at the interface and that the interfacial resistance was greater for films with significantly dissimilar interatomic potentials and/or with a greater degree of disorder at the interface. Molecular dynamics was also employed by Daly et al. [53, 54] to calculate the thermal conductivity of Ga As/Al As superlattices. Using a simplified model, they calculated the cross-plane thermal conductivity and attributed the reduction in thermal conductivity of superlattices with perfect interfaces to miniband formation [53]. In later work [54], they calculated the in-plane thermal conductivity of Ga As/Al As superlattices. Even for perfect interfaces, there was a 10–20% reduction in the superlattice thermal conductivity as compared with the individual conductivities of the two films. This was explained, for most cases, as a modification of the group velocity (dispersion curve) of the superlattice. When interfacial roughness was introduced, a large reduction in effective thermal conductivity was experienced and agreement with experimental data was shown.

2.3.5 Solid-Liquid Interfacial Regions. It is important to note that interfacial thermal resistance first became a topic of interest with the pioneering work of Kapitza [55] in 1941 who discovered the existence of a temperature jump across a low-temperature liquid-solid interface. Due to the increasingly critical role of the liquid-solid interface in systems of nanostructures, investigations of interfacial thermal transport across this type of interface are gaining attention. Various recent studies have utilized MD to explore this regime [56–59]. Of particular interest has been the enhancement in thermal conductivity experienced by a suspension of solid nanoparticles in a liquid [60]. Keblinski et al. [57] employed MD to help determine the significance of various mechanisms influencing thermal transport characteristics in these nanofluid systems. They demonstrated that within the nanoparticle, transport was ballistic and involved multiple scattering events with the solid/liquid interface. Furthermore, they showed that the characteristics of this interface significantly affected the transmission of phonons. Moreover, Huxtable et al. [59] experimentally measured the interface thermal conductance of carbon nanotubes suspended in surfactant micelles in water and compared their findings with a classical MD simulation. Their studies demonstrated that high-frequency phonon modes in the nanotubes undergo phonon-phonon scattering to generate low-frequency modes before being transmitted to the surroundings. They concluded that interface thermal conductance plays a very important role in determining the overall thermal conductivity of a network of nanotubes or of nanotubes embedded in a matrix material.

3 LASER-MATERIAL INTERACTIONS

3.1 Introduction

The interaction of lasers with solid materials is important in numerous applications including precision machining [61], medicine [62], thin-film deposition [63], and formation of carbon nanotubes [64]. Despite numerous analytical and experimental studies, much is still not understood about laser-material interaction and the resultant mechanisms of melting, vaporization, and ablation, particularly at picosecond time scales and below [65]. Recently, molecular dynamics simulation has been used to elucidate fundamental mechanisms of phase change [66] and thermomechanical phenomena [67] in laser-material interaction on a variety of materials including argon [66–69], silicon [70–75], carbon [76–79], metals [80–84], and organic materials [85]. Applications like laser thermal processing [74], phase change optical disks [86], and matrix-assisted laser desorption ionization mass spectrometry [87] have also been investigated using molecular dynamics. Other, earlier molecular dynamics studies of laser-material interaction are reviewed elsewhere [12, 13, 85, 88–90].

3.2 Implementation of Laser-Material Interaction in Molecular Dynamics Simulation

A key issue in molecular dynamics simulations of laser-material interactions is how to represent the excitation of the material by absorption of the electromagnetic wave. Below, the various mechanisms used to model the laser-material interaction are discussed.

3.2.1 Kinetic or Potential Energy Change. The simplest classical simulations typically neglect details of the absorption and model the interaction as a change in kinetic or potential energy of the molecules in the irradiated region. The kinetic energy addition is imposed by increasing the velocity of the irradiated atoms, while the potential energy change is manifested by using different potential energy curves for the irradiated atoms. Velocity rescaling is perhaps the simplest method of modeling the laser-material interaction, and has been widely used [83, 91]. Potential energy changes have also been implemented, for example by Kotake [92], and by Volz [68], who modeled absorption by argon of a photon in the case of no ablation or evaporation as a transition of a bound atom from its ground-state potential to an excited state potential energy curve.

3.2.2 Fictitious "Energy Carriers". Classical simulations with a slightly higher level of sophistication represent the laser-material interaction through the use of discrete "energy carriers" that propagate through the material [69, 74, 81]. These

carriers are neither photons nor electrons but rather are fictitious particles meant to model the lattice absorption as a discrete process. When an energy carrier collides with a molecule, the molecule absorbs its energy and undergoes an increase in kinetic energy. This method was initially introduced by Chokappa et al. [93] and later used by Wang et al. [74]. Kunugi et al. [81] modified this method by representing the carriers as "energy flux" particles that have energy but no mass, and they modeled the transport of these particles with Monte Carlo simulations. Perez and Lewis [69] modeled the irradiation as an exponentially decaying gas of carriers, which emit a "phonon" upon collision.

3.2.3 Classical Electron Gas. To model metallic materials in a more accurate manner than that provided by the "energy-carrier" approach above, particularly at short time scales, it is important to account for the excitation of electrons resulting from irradiation and the resulting transport of energy in the electronic system. Hakkinen et al. [82] incorporated electronic transport into molecular dynamics simulations of laser-material interaction by using the two-step heating model for metals [94, 95] and combining it with the embedded atom intermolecular potential. In the two-step model, laser energy is absorbed by the free electron gas, which is treated as a continuum. Electron-electron thermalization occurs on the time scale of tens of femtoseconds, after which time the electron gas can be characterized by a temperature. This temperature is initially different from the temperature of the lattice of ions, as the characteristic time for transfer of electronic energy to the lattice occurs on the order of a few picoseconds. After this time, both the electron and lattice temperatures are the same. To represent energy transfer from laser-heated electrons to the lattice, Hakkinen et al. used an electron lattice coupling term as an additional contribution to the ionic equations of motion. The coupling coefficient in this term is proportional to the electron-phonon coupling constant, the difference between electron and lattice temperatures, and the reciprocal of lattice specific heat. The temperature of the electron fluid is simulated classically using a numerical solution to the two-step model.

3.2.4 Discrete Electronic Carriers and Photons. At the next level of complexity in modeling laser-material interactions, all of the energy carriers, including photons, electrons, ions, and atoms, are modeled as discrete particles. Transfer of energy among the carriers occurs during collisions. Laser irradiation is modeled as individual photons in the material, most typically according to Lambert law absorption [71, 80] where the local number of photons decays exponentially into the material. Such an approach is problematic during ablation, however, since local removal of material creates areas of reduced absorption and thus results in variable local intensities. Herrmann et al. [73] addressed this issue by simulating the transport of individual photons in the material as a random process, using literature values for single- and two-photon probabilities to model the likelihood of photon absorption. Absorption has been manifested in the simulations by altering the intermolecular

potential [73,80] or by the generation of electron-hole pairs that diffuse and later recombine nonradiatively to generate lattice heating within a small region surrounding the recombination location [71,73].

3.2.5 Tight-Binding Methods. Tight-binding methods, as discussed above, offer the simplest way to introduce quantum-mechanical electronic effects into molecular dynamics simulations. Wang et al. [78] used a tight-binding model for carbon to investigate laser-induced graphitization of diamond for short (femtosecond) and long (nanosecond) laser pulses. The occupancy of the electronic states is described in both cases by the Fermi–Dirac distribution. For the nanosecond irradiation, they treat the electrons as being at the same temperature as the lattice. For femtosecond irradiation they assume the electrons to be at a much higher temperature than the lattice, and this temperature is kept constant throughout the simulation. In a series of papers, Jeschke and colleagues also investigate ultrashort pulse laser interactions with carbon, investigating graphitization of diamond [77], melting of C_{60} [76], and ablation of graphite films [96]. In these works, they employ more sophisticated modeling of the electronic temperature and occupancy than that by Wang et al. to describe the time dependence of the potential energy surfaces found at the laser-excited states. This is done by using the Boltzmann transport equation to describe the time evolution of the electronic energy level occupancy. The electronic temperature decay toward that of the lattice, caused by carrier diffusion and electron-phonon interactions, is modeled in a relaxation-time approach. Following Parrinello and Rahman [97], they also allow volume changes in their simulations. This allows part of the energy pumped into the system by the laser pulse to be spent as expansion/deformation, which is more physically realistic than constant volume simulations that overestimate the degree of ultrafast melting. Using this combination of approaches, they find agreement with the experimental data of others on ablation thresholds and thus demonstrate the validity of tight-binding methods for ultrafast studies on carbon. Two recent tight-binding studies on ultrafast silicon ablation by Jeschke et al. [70] and Gambirasio et al. [72] have also been reported. In contrast to the former paper, which uses the approach described immediately above, Gambirasio and coworkers assume a single unchanging electron temperature and incorporate two-photon absorption effects. Despite these differences in implementation, both studies show similarly good agreement between simulations and experiment [70], and simulations, experiment, and ab initio calculations [72].

3.2.6 Ab Initio Molecular Dynamics. The most rigorous way to model laser-material interaction is to apply ab initio simulation methods to this problem. Car-Parrinello molecular dynamics is only suitable for ground-state electrons, however, so Alavi et al. [98] developed an alternative density functional based molecular dynamics method that can treat systems with hot electrons. Silvestrelli and Parrinello [79] used this method to study laser-graphite interactions, and found that dramatic weakening of the covalent bond when electrons are sufficiently excited re-

sults in more rapid melting than that observed in their earlier simulations on silicon [99, 100]. They also observed qualitative agreement with experimental behavior observed at different laser fluences.

4 LIQUID-VAPOR INTERFACES

4.1 Introduction

The study of liquid-vapor interfaces is of critical importance in modern science and technology, and significant effort has been devoted to understanding interfacial structure and behavior in the past century. Due to the nanoscale thickness of the interfacial region, experimental observation of detailed interfacial behavior is exceedingly difficult. While an increasing number of experimental studies on liquid-vapor and particularly water-vapor interfaces (e.g., [101]) have appeared recently, statistical analysis and computer simulation methods are still widely used to gain insight into fundamental interfacial phenomena. Among these techniques, MD has proven to be a powerful and versatile tool. This section reviews recent developments in MD simulation of liquid-vapor interfaces, with a particular focus on surface tension and interfacial stability. Interfaces occur in planar (liquid film in vapor or vapor film in liquid), spherical (droplet or bubble), and cylindrical (liquid jet) geometries. The planar geometry is the simplest and for this reason the primary emphasis in the following sections is on planar interfaces, with the notion that most discussions there are also applicable to other geometries. The additional effects of curvature are also briefly discussed below. Detailed description of the simulation procedures can be found in recent review articles [12, 28] and references therein.

4.2 Previous Work

Since the early work of Chapela in the 1970s [102], tremendous progress has been made in MD simulation of liquid-vapor interfaces. This progress, in large part, has been driven by advances in computation. While most work in this area simulates monatomic LJ molecules [103–105], publications on MD simulation of polyatomic molecules interacting with complex potentials have emerged over the past few years. Examples include diatomic LJ molecules [106, 107], attractive hard-core Yukawa fluids [108], molten ionic solids [109, 110], water and aqueous solutions [111, 112], as well as organic molecules and polymers, such as dimethyl sulfoxide [113] and acetone [114].

4.3 Density Profile and Interface Thickness

The first step in simulating the liquid-vapor interface is to determine the density profile and from that the thickness of the interface. The typical density profile can be

expressed mathematically as [115]

$$\rho(z) = \frac{\rho_l + \rho_v}{2} - \frac{\rho_l - \rho_v}{2} \tanh \frac{2(z - z_e)}{d}, \tag{4}$$

where ρ_l and ρ_v refer to the liquid and vapor densities, respectively, z is a position coordinate measured from the center of the film, z_e indicates the position of the equimolar surface, and d is the interface thickness. All of these parameters can be obtained from numerical fitting. Although the simulation process is very straightforward, a great deal of physics is needed to interpret the result. There exist two contributions to the interface thickness: one from mass diffusion (evaporation and condensation), and the other from surface waves (since density is calculated by taking averages over time and space). According to the statistical theory of capillarity, the magnitude of the surface wave contribution depends on two factors: temperature, because the wave is thermally excited, and surface tension, which can be calculated from simulation separately. The size of the simulation domain also influences the surface wave because it determines the longest wavelength that can be represented in the simulation. This, however, is an artificial effect and should be decoupled from the simulation results. Since the calculated surface tension also depends on the choice of simulation domain, as discussed below, such decoupling still remains a challenge.

4.4 Surface Tension

It is of great interest to calculate surface tension and to predict its behavior under the influence of external parameters. For example, the van der Waals theory of capillarity indicates that surface tension vanishes on the approach to the critical point [115]

$$\gamma(T) \sim \left(1 - \frac{T}{T_c}\right)^{\mu}, \tag{5}$$

where T_c is the critical temperature. The many theoretical and numerical studies performed to obtain the exponent μ [115, 116] have shown that the exponent falls in the range $1.0 - 1.5$. In MD simulations, surface tension is typically calculated by integrating the local stress across the interface. Local stress is defined as the difference between the normal and tangential pressure components

$$\gamma = \int_0^{\infty} (P_N - P_T) dz. \tag{6}$$

In comparing the calculated surface tension with experimental data, it should be noted that a few parameters in the MD simulation procedure significantly affect the accuracy of prediction: cutoff radius and simulation domain size. In a homogeneous system, the choice of the cutoff radius is not very critical because long-range forces from all directions cancel each other. In interfacial studies where the local density changes by two orders of magnitude over a few nanometers, however, the choice of

the cutoff radius becomes important. Trokhymchuk and Alejandre [117] studied the effect of cutoff radius on surface tension as well as density profiles for a LJ liquid film. Their results indicate that the calculated value of surface tension increases as cutoff radius increases. Furthermore, the authors pointed out that the discrepancy between results from MD and Monte Carlo simulation (MC) is sometimes caused by the choice of insufficient cutoff radius. With a large cutoff radius, the discrepancy vanishes. Another factor that affects surface tension is the lateral dimension of the computational domain. All interfaces are subject to surface perturbations, which lead to surface waves. In the absence of gravity, the surface wave is then the capillary wave. Adopting the periodic boundary condition effectively excludes the existence of surface waves whose wavelengths are longer than the lateral dimension of the simulation domain L and increases the calculated surface tension. Both statistical analysis [118, 119] and MD simulation [110, 120] have shown that the calculated surface tension can be related to the surface tension of an infinitely large surface by

$$\gamma(L) - \gamma(\infty) = \frac{a \ln L}{L^2} . \tag{7}$$

Here a is a positive constant.

4.5 Local Stress and Thin-Film Stability

Recent MD simulations [105,109] have confirmed that the liquid-film thickness does not significantly affect the calculated surface tension. Further exploration of local stress profiles [105] suggests that the local stress is distributed differently in films of varying thickness (Figure 3). Typically, the local stress profile peaks at the interfacial region and decreases to zero in the bulk vapor and liquid regions where the pressure is isotropic (Figure 3a). At small film thicknesses, the simulations of Weng et al. [105] show that local stress does not return to zero at the center of a liquid film and that liquid molecules there are, in fact, under a finite tensile stress. In other words, the two interfacial regions at the two sides of a liquid film appear to overlap with each other. Local stress at the center increases as the film thickness decreases further (Figures 3b–d). When the film thickness falls below a critical value, liquid molecules cannot sustain the high tensile stress and film rupture occurs. Since the liquid phase can sustain more stress than vapor, one can conclude that the vapor film in liquid is less stable than the liquid film in vapor. Molecular dynamics simulation of vapor films has been performed to confirm this conclusion [121]. The interface overlapping phenomenon that appears in liquid films does not occur in vapor films, and the critical thickness for the vapor film is found to be 10% larger than that of the liquid film. This conclusion is contradictory to the analyses from classical thermodynamics. Thermodynamically, the critical thickness only depends on the computational domain size (the longest wavelength), surface tension, and the Hamaker constant, all of which are believed to be identical in these two cases.

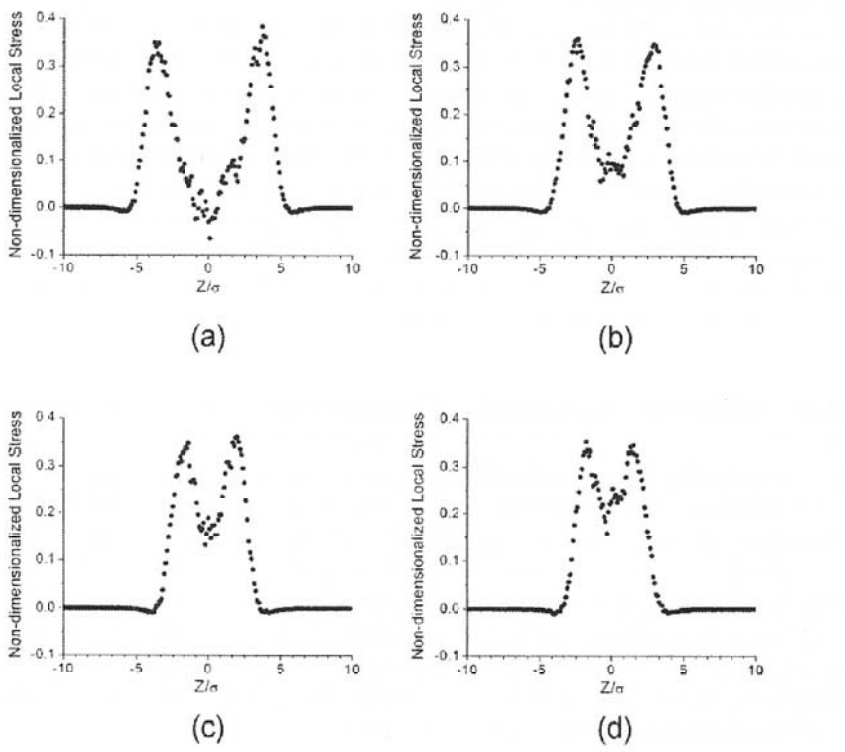

Figure 3 Nondimensional local stress as a function of film thickness: (a) thickest film, (b) thinner film, (c) still thinner film, and (d) thinnest film.

4.6 Multicomponent Systems

Understanding adsorption and distribution of foreign molecules at the liquid-vapor interface is critical to many chemical, physical, biological, and engineering problems. Its ability to reveal molecular-level structure makes MD simulation a valuable complement to experimental spectroscopic techniques [101,122,123] that have been applied to study interfacial phenomena. Numerous MD studies on this topic have been published in the past few years. Tomassone et al. [124] studied the dynamics of surfactants at liquid-vapor interfaces based on their solubility. Vieceli et al. [112] studied the vibrational energy exchange during the incidence of diatomic molecules on the water surface. Mountain [125] simulated the concentration profile of acetonitrile at the interface between vapor and the water-acetonitrile solution. Jungwirth and Tobias [126] investigated the distribution of ions at the water-vapor interface. In the modeling of multicomponent systems, identification of intermolecular forces between unlike species is very important. When the two species are both LJ type, two common methods are used to model their interactions. One method is to apply the Lorentz–Berthelot combination rule [127]. The other is to use the same energy

and length scales ε and σ to model like-like and like-unlike molecular interactions, but to introduce a parameter in the attractive term and vary this to modify like-unlike intermolecular attraction [124, 128]. For other types of molecules, such as water, the potential is modeled as the summation of the Coulomb interaction and an LJ potential [112]. Unlike the intermolecular interactions of LJ materials, the interactions in many other types of materials cannot be added pairwise and multibody effects must be considered. Another interesting issue is that, due to the limitation of computational power, in some simulations the cutoff radius is chosen to be relatively small. Although systematic studies on the effect of cutoff radius on surface tension and density profiles in LJ fluids have been performed [104, 117], such studies on Coulombic and other non-LJ systems are still lacking.

4.7 Spherical and Cylindrical Interfaces

Simulation work on liquid droplets in vapor started at about the same time as that on liquid films. One of the first papers in this area was published by Rusanov and Brodskaya in 1977 [129]. In contrast, MD simulations of vapor bubbles have appeared only in the past few years [130]. The major focus in MD studies of spherical interfaces has been to investigate the curvature effect on surface tension. Surface tension plays an important role in droplet condensation and bubble formation because the nucleation rate is an exponential function of surface tension. Thus, accurate prediction of surface tension is critical. Classically, the curvature effect is expressed mathematically by Tolman's equation [131, 132]

$$\frac{\gamma}{\gamma_\infty} = 1 - \frac{2\delta}{R_s} + \ldots, \tag{8}$$

where γ_∞ is the surface tension value for planar interfaces, δ is the Tolman length, and R_s is the radius of the surface of tension where the Young–Laplace equation applies

$$P_l - P_v = \frac{2\gamma}{R_s}. \tag{9}$$

Here P_l and P_v are the pressures inside the liquid drop and the bulk vapor, respectively. For bubbles, the two subscripts switch. It should be noted that the Tolman length depends on both temperature and curvature. Molecular dynamics simulation has shown that the Tolman length δ is positive for droplets and negative for bubbles, and has a value around or smaller than the LJ length parameter σ [130, 133], although a well-accepted value of the Tolman length is still not available because the simulation results depend strongly on the cutoff radius chosen in the simulation. Investigations utilizing the density functional theory of nucleation, however, report that δ decreases with increasing droplet radius and becomes negative when the droplet radius grows beyond a certain size [134, 135]. Molecular dynamics studies of cylindrical interfaces have primarily focused on the stability condition of liquid jets in vapor. In the study of rupture time for stationary, infinitely long, circular, incompressible

liquid jets, qualitative agreement was found between MD simulation and prediction from the Rayleigh's classical study on linear stability [136, 137]. For liquid jets that are extruded from a nozzle, Moseler and Landman's simulation indicated that thermal fluctuations play an increasingly important role on the breakup condition as the jet radius approaches the nanoscale, and failure to include the fluctuation effect causes the classical hydrodynamic model to disagree with MD simulation [138]. It should also be noted that as the jet radius fluctuates, the local surface tension will change due to the curvature effect, and this effect is not considered in the classical treatment.

5 CONCLUSIONS

Molecular dynamics simulation offers a microscopic route to understanding the fundamental thermophysical mechanisms that influence thermal transport in nanostructures and molecules, short-time-scale laser-material interactions, and liquid-vapor interfacial phenomena. Application of molecular dynamics to these areas has resulted in several important advances over the past five years. The size and temperature dependence of the thermal conductivity of nanostructures and carbon nanotubes has been explored, typically revealing increases in thermal conductivity with increasing characteristic dimension. For nanowires, comparison of MD to other thermal conductivity calculation methods, such as the Boltzmann transport equation and the equation of phonon radiative transfer, suggests that specularity parameters lie in the 0.35 – 0.45 range. Parameters, such as interfacial strain and superlattice layer thickness, have been investigated and demonstrated to play a significant role in superlattice thermal transport. Recent work on nanofluid systems indicates that interface quality and scattering of high-frequency phonons within the solid influence thermal transport across the solid-liquid interface and may also be important for thermal conduction in nanocomposite materials. Various methods for modeling laser-material interaction have been implemented, including changing the kinetic and/or potential energy of the irradiated atoms, utilizing the two-step heating model for metals to model the electron gas as a continuum, representing the atoms and electrons as discrete particles and modeling their interactions using Monte Carlo and Boltzmann transport equation techniques, and using semiempirical and ab initio quantum-mechanical methods. Metrics based on the Boltzmann H function and the translational order parameter of Verlet have been introduced as a convenient method to determine whether a simulation has reached steady state, which can be difficult and computationally burdensome to ascertain in nonequilibrium simulations using other techniques, such as monitoring particle velocity distributions. In the liquid-vapor literature, there is much current interest in the simulation of interfacial phenomena in diatomic, ionic, organic, and other complex fluids. For LJ fluids, MD simulations have demonstrated that surface tension increases with cutoff radius, but displays little dependence on liquid-film thickness. Calculations of local stresses indicate that the increasing overlap of liquid-vapor interfaces as liquid film thickness is reduced leads to high tensile stresses at the center of the film that result in film rupture. Classical predictions for

the breakup of cylindrical liquid jets neglect the important influence of thermal fluctuations, which have been shown by MD to become increasingly important as jet size decreases to the nanoscale.

6 FUTURE DIRECTIONS

The studies above highlight numerous directions for future work in the MD simulation of nanoscale thermophysical phenomena. More studies to clarify and quantify the effect of acoustic impedance and phonon spectra mismatch, miniband formation, group velocity reduction, phonon tunneling, and lattice strain on thermal conductivity would greatly benefit the understanding of thermal transport in nanostructures. Of particular interest is specific information regarding phonon-interface scattering. Initial strides in this direction have been made by Schelling et al. [139], who employed MD to illustrate dynamic phonon propagation and interfacial scattering events occurring at an ideal semiconductor-semiconductor interface. Interestingly, the transmission coefficients calculated from the investigation compare favorably with the acoustic mismatch model, but only for large wavelengths. Further investigation along these lines would help clarify the reasons for this wavelength dependence. Additional work to elucidate the disparities in magnitude and peak temperature dependence of carbon nanotube thermal conductivity simulated by various researchers should also be performed. It is not clear whether the calculated peaks have a physical basis or are an artifact of the finite simulation domain, and new studies would provide much information. Wider utilization of semiempirical techniques, such as tight binding, which account for quantum effects in a computationally manageable way, are a key direction for future laser-material interaction studies. For liquid-vapor interfacial studies, a few fundamental issues should be addressed in the near future. The first issue is related to the cutoff radius. Although the sophistication of fluid models continues to increase, systematic investigation of the effect of cutoff radius, and therefore of long-range forces, on surface tension and density profile is still not available for many complex fluids. If computational power advances in the near future do not allow sufficient expansion of cutoff radius, statistical methods should be developed to determine the long-range force correction. Surface tension calculation will remain a key topic, as it is the most important property of an interface in a single-component system. In multicomponent systems, there exist many different important phenomena that require further MD study, including the orientation of foreign organic molecules at liquid-vapor interfaces, which is critical to understanding Langmuir–Blodgett film deposition, and diffusion of foreign molecules from one phase to the other, which is important in biological and chemical reactions. For spherical interfaces, the Tolman length will likely continue to be a focus of investigation. The dependence of Tolman length on temperature, intermolecular potential, and interface curvature still needs to be unambiguously quantified. In addition to studies on droplets, the nanoscale interfacial phenomena in bubbles should also receive more research attention.

ACKNOWLEDGMENTS

J. R. Lukes is supported by the Office of Naval Research (N00014-03-1-0890).

REFERENCES

1. M. E. Tuckerman and G. J. Martyna, Understanding Modern Molecular Dynamics: Techniques and Applications, *J. Phys. Chem. B*, Vol. 104, pp. 159–178, 2000.
2. D. R. Hartree, The Wave Mechanics of an Atom with a Non-Coulomb Central Field. Part I. Theory and Methods, *Proc. Cambridge Philos. Soc.*, Vol. 24, pp. 89–110, 1928.
3. D. R. Hartree, The Wave Mechanics of an Atom with a Non-Coulomb Central Field. Part II. Some Results and Discussion, *Proc. Cambridge Philos. Soc.*, Vol. 24, pp. 111–132, 1928.
4. V. A. Fock, Naherungsmethode zur Losung der Quantenmechanischen Mehrkorperproblems, *Z. Phys.*, Vol. 61, pp. 126–148, 1930.
5. P. Hohenberg and W. Kohn, Inhomogeneous Electron Gas, *Phys. Rev.*, Vol. 136, pp. B864–B871, 1964.
6. W. Kohn and L. J. Sham, Self-Consistent Equations Including Exchange and Correlation Effects, *Phys. Rev.*, Vol. 140, pp. A1133–A1138, 1965.
7. E. Wimmer, Computational Materials Design and Processing: Perspectives for Atomistic Approaches, *Mater. Sci. Eng. B*, Vol. 37, pp. 72–82, 1996.
8. R. Car and M. Parrinello, Unified Approach for Molecular Dynamics and Density-Functional Theory, *Phys. Rev. Lett.*, Vol. 55, pp. 2471–2474, 1985.
9. M. J. S. Dewar and W. Thiel, Ground States of Molecules, 38: The MNDO Method. Approximations and Parameters, *J. Am. Chem. Soc.*, Vol. 99, pp. 4899–4907, 1977.
10. J. C. Slater and G. F. Koster, Simplified LCAO Method for the Periodic Potential Problem, *Phys. Rev.*, Vol. 94, pp. 1498–1524, 1954.
11. R. Car, Introduction to Density-Functional Theory and Ab-Initio Molecular Dynamics, *Quant. Struct.-Activity Relation.*, Vol. 21, pp. 97–104, 2002.
12. S. Maruyama, Molecular Dynamics Method for Microscale Heat Transfer, in: *Advances In Numerical Heat Transfer*, W. J. Minkowycz and E. M. Sparrow, Eds, Taylor & Francis, New York, Vol. 2, pp. 189–226, 2000.
13. F.-C. Chou, J. R. Lukes, X.-G. Liang, K. Takahashi, and C.-L. Tien, Molecular Dynamics in Microscale Thermophysical Engineering, *Ann. Rev. Heat Transfer*, Vol. 10, pp. 141–176, 1999.
14. U. Burkert and N. L. Allinger, *Molecular Mechanics*, American Chemical Society, Washington, DC, 1982.
15. M. Born and K. Huang, *Dynamical Theory of Crystal Lattices*, Clarendon Press, Oxford, 1954.
16. N. Metropolis and S. Ulam, The Monte Carlo Method, *J. Am. Stat. Assoc.*, Vol. 44, pp. 335–341, 1949.
17. K. Binder, ed., *Monte Carlo Methods in Statistical Physics*, Springer-Verlag, Berlin, 1984.
18. M. P. Allen and D. J. Tildesley, *Computer Simulation of Liquids*, Clarendon Press, Oxford, 1987.

19. J. M. Haile, *Molecular Dynamics Simulation: Elementary Methods*, Wiley, New York, 1992.
20. D. C. Rapaport, *The Art of Molecular Dynamics Simulation*, Cambridge University Press, Cambridge, 1995.
21. F. H. Stillinger and T. A. Weber, Computer Simulation of Local Order in Condensed Phases of Silicon, *Phys. Rev. B*, Vol. 31, pp. 5262–5271, 1985.
22. D. W. Brenner, Empirical Potential for Hydrocarbons for use in Simulating the Chemical Vapor Deposition of Diamond Films, *Phys. Rev. B*, Vol. 42, pp. 9458–9471, 1990.
23. M. S. Daw and M. I. Baskes, Embedded-Atom Method: Derivation and Application to Impurities, Surfaces, and Other Defects in Metals, *Phys. Rev. B*, Vol. 29, pp. 6443–6453, 1984.
24. F. W. Finnis and J. E. Sinclair, A Simple Empirical N-Body Potential for Transition Metals, *Philos. Mag. A*, Vol. 50, pp. 45–55, 1984.
25. H. J. C. Berendsen, J. R. Grigera, and T. P. Straatsma, The Missing Term in Effective Pair Potentials, *J. Phys. Chem.*, Vol. 91, pp. 6269–6271, 1987.
26. W. L. Jorgenson, J. Chandrasekhar, J. D. Madura, R. W. Impey and M. L. Klein, Comparison of Simple Potential Functions for Simulating Liquid Water, *J. Chem. Phys.*, Vol. 79, pp. 926–935, 1983.
27. R. Car, Modeling Materials by Ab-Initio Molecular Dynamics, in: *Quantum Theory of Real Materials*, J. R. Chelikowsky and S.G. Louie, Eds, Kluwer Academic Publishers, Norwell, pp. 23–37, 1996.
28. C.-L. Tien and J.-G. Weng, Molecular Dynamics Simulation of Nanoscale Interfacial Phenomena in Fluids, *Adv. Appl. Mech.*, Vol. 38, pp. 95–146, 2001.
29. R. Kubo, Statistical Mechanical Theory of Irreversible Processes. I. General Theory and Simple Applications to Magnetic and Conduction Problems, *J. Phys. Soc. Jap.*, Vol. 12, pp. 570–586, 1957.
30. D. P. Hansen and D. J. Evans, A Generalized Heat Flow Algorithm, *Mol. Phys.*, Vol. 81, pp. 767–779, 1994.
31. M. J. Gillan and M. Dixon, The Calculation of Thermal Conductivities by Perturbed Molecular Dynamics Simulation, *J. Phys. C*, Vol. 16, pp. 869–878, 1983.
32. J. R. Lukes, D. Y. Li, X.-G. Liang, and C.-L. Tien, Molecular Dynamics Study of Solid Thin-Film Thermal Conductivity, *J. Heat Transfer*, Vol. 122, pp. 536–543, 2000.
33. H. Xue and C. Shu, Equilibration of Heat Conduction Simulation in a Very Thin Film Using Molecular Dynamics, *Int. J. Numer. Methods Heat Fluid Flow*, Vol. 9, pp. 60–71, 1999.
34. L. Verlet, Computer "Experiments" on Classical Fluids. I. Thermodynamical Properties of Lennard – Jones Molecules, *Phys. Rev.*, Vol. 159, pp. 98–103, 1967.
35. S. Volz and G. Chen, Molecular Dynamics Simulation of Thermal Conductivity of Silicon Nanowires, *Appl. Phys. Lett.*, Vol. 75, pp. 2056–2058, 1999.
36. X. Lu and J. H. Chu, Phonon Heat Transport in Silicon Nanowires, *Eur. Phys. J. B*, Vol. 26, pp. 375–378, 2002.
37. X. Lu, W. Z. Shen, and J. H. Chu, Size Effect on the Thermal Conductivity of Nanowires, *J. Appl. Phys.*, Vol. 91, pp. 1542–1552, 2002.
38. J. Tersoff, New Empirical Approach for the Structure and Energy of Covalent Systems, *Phys. Rev. B*, Vol. 37, pp. 6991–7000, 1988.
39. J. Hone, M. Whitney, C. Piskotti, and A. Zettl, Thermal Conductivity of Single-

Walled Carbon Nanotubes, *Phys. Rev. B*, Vol. 59, pp. R2514–R2516, 1999.
40. M. A. Osman and D. Srivastava, Temperature Dependence of the Thermal Conductivity of Single-Wall Carbon Nanotubes, *Nanotechnology*, Vol. 12, pp. 21–24, 2001.
41. D. Li, Y. Wu, P. Kim, L. Shi, P. Yang, and A. Majumdar, Thermal Conductivity of Individual Silicon Nanowires, *Appl. Phys. Lett.*, Vol. 83, pp. 2934–2936, 2003.
42. S. Berber, Y. K. Kwon and D. Tomanek, Unusually High Thermal Conductivity of Carbon Nanotubes, *Phys. Rev. Lett.*, Vol. 84, pp. 4613–4616, 2000.
43. D. J. Evans, Homogeneous NEMD Algorithm for Thermal Conductivity – Application of Non-Canonical Linear Response Theory, *Phys. Lett.*, Vol. 91A, pp. 457–460, 1982.
44. S. Maruyama, A Molecular Dynamics Simulation of Heat Conduction of a Finite Length Single-Walled Carbon Nanotube, *Microscale Thermophys. Eng.*, Vol. 7, pp. 41–50, 2003.
45. J. Che, T. Cagin, and W. A. Goddard III, Thermal Conductivity of Carbon Nanotubes, *Nanotechnol.*, Vol. 11, pp. 65–69, 2000.
46. X. G. Liang and B. Shi, Two-Dimensional Molecular Dynamics Simulation of the Thermal Conductance of Superlattices, *Mater. Sci. Eng. A*, Vol. 292, pp. 198–202, 2000.
47. S. Volz, J.-B. Saulnier, G. Chen, and P. Beauchamp, Computation of Thermal Conductivity of Si/Ge Superlattices by Molecular Dynamics Techniques, *Microelectron. J.*, Vol. 31, pp. 815–819, 2000.
48. S. Volz, J.-B. Saulnier, G. Chen, and P. Beauchamp, Molecular Dynamics of Heat Transfer in Si/Ge Superlattices, *High Temp.–High Pres.*, Vol. 32, pp. 709–714, 2000.
49. A. R. Abramson, C.-L. Tien, and A. Majumdar, Interface and Strain Effects on the Thermal Conductivity of Heterostructures: A Molecular Dynamics Study, *J. Heat Transfer*, Vol. 124, pp. 963–970, 2002.
50. R. C. Picu, T. Borca-Tasciuc, and M. C. Pavel, Strain and Size Effects on Heat transport in Nanostructures, *J. Appl. Phys.*, Vol. 93, pp. 3535–3539, 2003.
51. J. K. Yang, Y. F. Chen, and J. P. Yan, Molecular Dynamics Simulation of Thermal Conductivities of Superlattice Nanowires, *Sci. China, Ser. E*, Vol. 46, pp. 278–286, 2003.
52. C. J. Twu and J. R. Ho, Molecular-Dynamics Study of Energy Flow and the Kapitza Conductance Across an Interface with Imperfection Formed by Two Dielectric Thin Films, *Phys. Rev. B*, Vol. 67, pp. 205–422, 2003.
53. B. C. Daly, H. J. Maris, K. Imamura, and S. Tamura, Molecular Dynamics Calculation of the Thermal Conductivity of Superlattices, *Phys. Rev. B*, Vol. 66, pp. 024–301, 2002.
54. B. C. Daly, H. J. Maris, Y. Tanaka, and S. Tamura, Molecular Dynamics Calculation of the In-Plane Thermal Conductivity of Ga As/Al As Superlattices, *Phys. Rev. B*, Vol. 67, pp. 033–308, 2003.
55. P. L. Kapitza, The Studey of Heat Transfer in Helium II, *J. Phys. USSR*, Vol. 4, pp. 181–210, 1941.
56. T. Ohara and D. Suzuki, Intermolecular Energy Transfer at a Solid-Liquid Interface, *Microscale Themophys. Eng.*, Vol. 4, pp. 189–196, 2000.
57. P. Keblinski, S. R. Phillpot, S. U. S. Choi, and J. A. Eastman, Mechanisms of Heat Flow in Suspensions of Nano-Sized Particles (Nanofluids), *Int. J. Heat Mass*

Transfer, Vol. 45, pp. 855–863, 2002.

58. L. Xue, P. Keblinski, S. R. Phillpot, S. U.-S. Choi, and J. A. Eastman, Two Regimes of Thermal Resistance at a Liquid-Solid Interface, *J. Chem. Phys.*, Vol. 118, pp. 337–339, 2003.
59. S. T. Huxtable, D. G. Cahill, S. Shenogin, L. Xue, R. Ozisik, P. Barone, M. Usrey, M. S. Strano, G. Siddons, M. Shim, and P. Keblinski, Interfacial Heat flow in Carbon Nanotube Suspensions, *Nature Mater.*, Vol. 2, pp. 731–734, 2003.
60. S. U. S. Choi, Enhancing Thermal Conductivity of Fluids with Nanoparticles, in: *Proc. Int. Mech. Eng. Congr. and Expos.*, San Francisco, FRD-Vol. 231, pp. 99–105, 1995.
61. G. Chryssolouris, N. Anifantis, and S. Karagiannis, Laser Assisted Machining: An Overview, *J. Manuf. Sci. Eng.*, Vol. 119, pp. 766–769, 1997.
62. B. Jean and T. Bende, Mid-IR Laser Applications in Medicine, *Topics Appl. Phys.*, Vol. 89, pp. 511–544, 2003.
63. I. W. Boyd, Thin Film Growth by Pulsed Laser Deposition, *Ceramics Int.*, Vol. 22, pp. 429–434, 1996.
64. A. Thess, R. Lee, P. Nikolaev, H. Dai, P. Petit, J. Robert, C. Xu, Y. Hee Lee, S. Gon Kim, A. G. Rinzler, D. T. Colbert, G. E. Scuseria, D. Tomanek, J. E. Fischer, and R. E. Smalley, Crystalline Ropes of Metallic Carbon Nanotubes, *Science*, Vol. 273, pp. 483–487, 1996.
65. K. Sokolowski-Tinten, J. Bialkowski, A. Cavalleri and D. von der Linde, Transient States of Matter during Short Pulse Laser Ablation, *Phys. Rev. Lett.*, Vol. 81, pp. 224–227, 1998.
66. X. Wang and X. Xu, Molecular Dynamics Simulation of Heat Transfer and Phase Change during Laser Material Interaction, *J. Heat Transfer*, Vol. 124, pp. 265–274, 2002.
67. X. Wang and X. Xu, Molecular Dynamics Simulation of Thermal and Thermomechanical Phenomena in Picosecond Laser Material Interaction, *Int. J. Heat Mass Transfer*, Vol. 46, pp. 45–53, 2003.
68. S. Volz, M. Lallemand, B. Perrin, and P. Depondt, Molecular Dynamics Study of Thermal and Acoustic Effects Generated by a Subpicosecond Laser Pulse Applied to a Thin Film, *High Temp. – High Pres.*, Vol. 30, pp. 607–612, 1998.
69. D. Perez and L. J. Lewis, Ablation of Solids under Femtosecond Laser Pulses, *Phys. Rev. Lett.*, Vol. 89, pp. 255–504, 2002.
70. H. O. Jeschke, M. E. Garcia, M. Lenzner, J. Bonse, J. Kruger, and W. Kautek, Laser Ablation Thresholds of Silicon for Different Pulse Durations: Theory and Experiment, *Appl. Surf. Sci.*, Vol. 197–198, pp. 839-844, 2002.
71. P. Lorazo, L. J. Lewis, and M. Meunier, Picosecond Pulsed Laser Ablation of Silicon: A Molecular-Dynamics Study, *Appl. Surf. Sci.*, Vol. 168, pp. 276–279, 2000.
72. A. Gambirasio, M. Bernasconi, and L. Colombo, Laser-Induced Melting of Silicon: A Tight-Binding Molecular Dynamics Simulation, *Phys. Rev. B*, Vol. 61, pp. 8233–8237, 2000.
73. R. F. W. Herrmann, J. Gerlach, and E. E. B. Campbell, Ultrashort Pulse Laser Ablation of Silicon: an MD Simulation Study, *Appl. Phys. A*, Vol. 66, pp. 35–42, 1998.
74. L. Wang, P. Clancy, M. O. Thompson, and C. S. Murthy, Thermodynamic and Kinetic Studies of Laser Thermal Processing of Heavily Boron-doped Amorphous Silicon Using Molecular Dynamics, *J. Appl. Phys.*, Vol. 92, pp. 2412–2419, 2002.

75. Y. Ishizaka, K. Watanabe, I. Fukumoto, E. Ohmura, and I. Miyamoto, Three-Dimensional Molecular Dynamics Simulation on Laser Materials Processing of Silicon, in: *ICALEO'98: Proc. Laser Materials Processing Conf.*, Laser Inst. of America, Orlando, 85, pp. 55–63, 1998.
76. H. O. Jeschke, M. E. Garcia, and K. H. Bennemann, Theory for Laser-Induced Ultrafast Phase Transitions in Carbon, *Appl. Phys. A*, Vol. 69, pp. S49–S53, 1999.
77. H. O. Jeschke, M. E. Garcia, and K. H. Bennemann, Microscopic Analysis of the Laser-Induced Femtosecond Graphitization of Diamond, *Phys. Rev. B*, Vol. 60, pp. R3701–R3704, 1999.
78. C. Z. Wang, K. M. Ho, M. D. Shirk, and P. A. Molian, Laser-Induced Graphitization on a Diamond (111) Surface, *Phys. Rev. Lett.*, Vol. 85, pp. 4092–4095, 2000.
79. P. L. Silvestrelli and M. Parrinello, Ab Initio Molecular Dynamics Simulation of Laser Melting of Graphite, *J. Appl. Phys.*, Vol. 83, pp. 2478–2483, 1998.
80. P. A. Atanasov, N. N. Nedialkov, S. E. Imomova, A. Ruf, H. Hugel, F. Dausinger, and P. Berger, Laser Ablation of Ni by Ultrashort Pulses: Molecular Dynamics Simulation, *Appl. Surf. Sci.*, Vol. 186, pp. 369–373, 2002.
81. T. Kunugi and K. Ezato, Numerical Analysis of Melting and Evaporation Behavior of a Molybdenum Layer Irradiated with a Laser Beam, *Heat Transfer–Jap. Res.*, Vol. 24, pp. 255–271, 1995.
82. H. Hakkinen and U. Landman, Superheating, Melting, and Annealing of Copper Surfaces, *Phys. Rev. Lett.*, Vol. 71, pp. 1023–1026, 1993.
83. Y. Dou, L. V. Zhigilei, Z. Postawa, N. Winograd, and B. J. Garrison, Thickness Effects of Water Overlayer on its Explosive Evaporation at Heated Metal Surfaces, *Nucl. Instrum. Methods Phys. Res. B*, Vol. 180, pp. 105–111, 2001.
84. E. Ohmura, I. Fukumoto, and I. Miyamoto, Molecular Dynamics Simulation on Laser Ablation and Thermal Shock Phenomena, in: *ICALEO '98: Proc. Laser Materials Processing Conf.*, Laser Inst. of America, Orlando, 85, pp. 45–54, 1998.
85. L. V. Zhigilei, E. Leveugle, B. J. Garrison, Y. G. Yingling, and M. I. Zeifman, Computer Simulations of Laser Ablation of Molecular Substrates, *Chem. Rev.*, Vol. 103, pp. 321–347, 2003.
86. T. Inoue and T. Uehara, Phase Transformation and Related Thermo-Mechanical Behaviour. A Molecular Dynamics Approach, *J. Phys. IV*, Vol. 9, pp. Pr9_341–Pr9_349, 1999.
87. L. V. Zhigilei, Y. G. Yingling, T. E. Itina, T. A. Schoolcraft, and B. J. Garrison, Molecular Dynamics Simulations of Matrix-Assisted Laser Desorption-Connections to Experiment, *Int. J. Mass Spectrom.*, Vol. 226, pp. 85–106, 2003.
88. S. Kotake, Future Aspects of Molecular Heat and Mass Transfer Studies, in: *Microscale and Molecular Heat Transfer*, S. Kotake and C.-L. Tien, Eds, Begell House, New York, pp. 12–20, 1994.
89. T. Ohara, Molecular Dynamics Study in Microscale Thermophysical Engineering: Current Activities and Future in Japan, *Microscale Thermophys. Eng.*, Vol. 4, pp. 213–221, 2000.
90. D. Poulikakos, S. Arcidiacono, and S. Maruyama, Molecular Dynamics Simulation in Nanoscale Heat Transfer: A Review, *Microscale Thermophys. Eng.*, Vol. 7, pp. 181–206, 2003.
91. J. I. Etcheverry and M. Mesaros, Molecular Dynamics Simulation of the Production of Acoustic Waves by Pulsed Laser Irradiation, *Phys. Rev. B*, Vol. 60, pp. 9430–9434, 1999.

92. S. Kotake, Molecular Dynamics Study of Solid Melting and Vaporization by Laser Irradiation, *Int. J. Heat Mass Transfer*, Vol. 36, pp. 2061–2067, 1993.
93. D. K. Chokappa and P. Clancy, The Influence of an Interface in the Promotion of Melting, *Mol. Phys.*, Vol. 65, pp. 97–107, 1988.
94. T. Q. Qiu and C.-L. Tien, Short-Pulse Laser Heating on Metals, *Int. J. Heat Mass Transfer*, Vol. 35, pp. 719–726, 1992.
95. S. I. Anisimov, D. L. Kapeliovich, and T. L. Perel'man, Electron Emission from Metal Surfaces Exposed to Ultrashort Laser Pulses, *Sov. Phys. JETP*, Vol. 39, pp. 375–377, 1974.
96. H. O. Jeschke, M. E. Garcia, and K. H. Bennemann, Theory for the Ultrafast Ablation of Graphite Films, *Phys. Rev. Lett.*, Vol. 87, pp. 015003, 2001.
97. M. Parrinello and A. Rahman, Polymorphic Transitions in Single Crystals: A New Molecular Dynamics Method, *J. Appl. Phys.*, Vol. 52, pp. 7182–7190, 1981.
98. A. Alavi, J. Kohanoff, M. Parrinello, and D. Frenkel, Ab Initio Molecular Dynamics with Excited Electrons, *Phys. Rev. Lett.*, Vol. 73, pp. 2599–2602, 1994.
99. P. L. Silvestrelli, A. Alavi, M. Parrinello, and D. Frenkel, Ab Initio Molecular-Dynamics Simulation of Laser Melting of Silicon, *Phys. Rev. Lett.*, Vol. 77, pp. 3149–3152, 1996.
100. P. L. Silvestrelli, A. Alavi, M. Parrinello, and D. Frenkel, Structure, Dynamical, Electronic, and Bonding Properties of Laser-Heated Silicon: An Ab Initio Molecular-Dynamics Study, *Phys. Rev. B*, Vol. 56, pp. 3806–3812, 1997.
101. A. M. Tikhonov and M. L. Schlossman, Surfactant and Water Ordering in Triacontanol Monolayers at the Water-Hexane Interface, *J. Phys. Chem. B*, Vol. 107, pp. 3344–3347, 2003.
102. G. A. Chapela, G. Saville, S. M. Thompson, and J. S. Rowlinson, Computer Simulation of a Gas-Liquid Surface, *J. Chem. Soc., Faraday Trans. II*, Vol. 73, pp. 1133–1144, 1977.
103. M. J. P. Nijmeijer, A. F. Bakker, C. Bruin, and J. H. Sikkenk, A Molecular Dynamics Simulation of the Lennard–Jones Liquid-Vapor Interface, *J. Chem. Phys.*, Vol. 89, pp. 3789–3792, 1988.
104. M. Mecke, J. Winkelmann, and J. Fischer, Molecular Dynamics Simulation of the Liquid-Vapor Interface: The Lennard–Jones Fluid, *J. Chem. Phys.*, Vol. 107, pp. 9264, 1997.
105. J.-G. Weng, S. Park, J. R. Lukes, and C.-L. Tien, Molecular Dynamics Investigation of Thickness Effect on Liquid Films, *J. Chem. Phys.*, Vol. 113, pp. 5917–5923, 2000.
106. M. Mecke, J. Fischer, and J. Winkelmann, Molecular Dynamics Simulation of the Liquid-Vapor Interface of Dipolar Fluids under Different Electrostatic Boundary Conditions, *J. Chem. Phys.*, Vol. 114, pp. 5842–5852, 2001.
107. J. Alejandre, Y. Duda, and S. Sokolowski, Computer Modeling of the Liquid-Vapor Interface of an Associating Lennard–Jones Fluid, *J. Chem. Phys.*, Vol. 118, pp. 329–336, 2003.
108. M. Gonzalez-Melchor, A. Trokhymchuk, and J. Alejandre, Surface Tension at the Vapor-Liquid Interface in an Attractive Hard-Core Yukawa Fluid, *J. Chem. Phys.*, Vol. 115, pp. 3862–3872, 2001.
109. A. Aguado, M. Wilson, and P. A. Madden, Molecular Dynamics Simulations of the Liquid-Vapor Interface of a Molten Salt. I. Influence of the Interaction Potential, *J. Chem. Phys.*, Vol. 115, pp. 8603–8611, 2001.

110. A. Aguado, W. Scott, and P. A. Madden, Molecular Dynamics Simulations of the Liquid-Vapor Interface of a Molten Salt. II. Finite Size Effects and Comparison to Experiment, *J. Chem. Phys.*, Vol. 115, pp. 8612–8619, 2001.
111. L. L. Vasiliev, D. Khrustalev, S. Konev, and M. Rabetsky, Heat Pipes for Electronic Equipment Cooling Systems, in: *Proc. 7th Int. Heat Pipe Conf.*, Minsk, USSR, 1990.
112. J. Vieceli, I. Chorny, and I. Benjamin, Vibrational Relaxation at Water Surfaces, *J. Chem. Phys.*, Vol. 117, pp. 4532–4541, 2002.
113. S. Senapati, A Molecular Dynamics Simulation Study of the Dimethyl Sulfoxide Liquid-Vapor Interface, *J. Chem. Phys.*, Vol. 117, pp. 1812–1816, 2002.
114. Y. L. Yeh, C. Zhang, H. Held, A. M. Mebel, X. Wei, S. H. Lin, and Y. R. Shen, Structure of the Acetone Liquid-Vapor Interface, *J. Chem. Phys.*, Vol. 114, pp. 1837–1843, 2001.
115. J. S. Rowlinson and B. Widom, *Molecular Theory of Capillarity*, Clarendon Press, Oxford, 1982.
116. V. P. Carey, Thermodynamic Properties and Structure of the Liquid-Vapor Interface: A Neoclassical Redlich–Kwong Model, *J. Chem. Phys.*, Vol. 118, pp. 5053–5064, 2003.
117. A. Trokhymchuk and J. Alejandre, Computer Simulations of Liquid-Vapor Interface in Lennard–Jones Fluids: Some Questions and Answers, *J. Chem. Phys.*, Vol. 111, pp. 8510–8523, 1999.
118. K. Binder, Monte Carlo Calculation of the Surface Tension for Two- and Three-Dimensional Lattice-Gas Models, *Phys. Rev. A*, Vol. 25, pp. 1699–1709, 1982.
119. J. J. Potoff and A. Z. Panagiotopoulos, Surface Tension of the Three-Dimensional Lennard–Jones Fluid from Histogram-Reweighting Monte Carlo Simulations, *J. Chem. Phys.*, Vol. 112, pp. 6411, 2000.
120. L.-J. Chen, Area Dependence of the Surface Tension of a Lennard–Jones Fluid from Molecular Dynamics Simulations, *J. Chem. Phys.*, Vol. 103, pp. 10214, 1995.
121. J.-G. Weng, C.-L. Tien, and A. Majumdar, Intermolecular and Surface Forces and their Role in Nanoscale Liquid Transport and Phase Change, in: *ASME Int. Mech. Eng. Conf. and Expos.*, ASME, New York, 2001.
122. A. Tojima, T. Manaka, and M. Iwamoto, Orientation Order Study of Monolayers at the Air-Water Interface by Maxwell-Displacement Current and Optical Second Harmonic Generation, *J. Chem. Phys.*, Vol. 115, pp. 9010–9017, 2001.
123. A. V. Benderskii and K. B. Eisenthal, Aqueous Solvation Dynamics at the Anionic Surfactant Air-Water Interface, *J. Phys. Chem. B*, Vol. 105, pp. 6698–6703, 2001.
124. M. S. Tomassone, A. Couzis, C. M. Maldarelli, J. R. Banavar, and J. Koplik, Molecular Dynamics Simulation of Gaseous-Liquid Phase Transitions of Soluble and Insoluble Surfactants at a Fluid Interface, *J. Chem. Phys.*, Vol. 115, pp. 8634–8642, 2001.
125. R. D. Mountain, Molecular Dynamics Study of Thin Water-Acetonitrile Films, *J. Phys. Chem. B*, Vol. 105, pp. 6556–6561, 2001.
126. P. Jungwirth and D. J. Tobias, Ions at the Air-Water Interface, *J. Phys. Chem. B*, Vol. 106, pp. 6361–6373, 2002.
127. M. Mecke, J. Winkelmann, and J. Fischer, Molecular Dynamics Simulation of the Liquid-Vapor Interface: Binary Mixtures of Lennard–Jones Fluids, *J. Chem. Phys.*, Vol. 110, pp. 1188, 1999.
128. E. Diaz-Herrera, J. Alejandre, G. Ramirez-Santiago, and F. Forstmann, Interfacial

Tension Behavior of Binary and Ternary Mixtures of Partially Miscible Lennard–Jones Fluids: A Molecular Dynamics Simulation, *J. Chem. Phys.*, Vol. 110, pp. 8084–8089, 1999.

129. A. I. Rusanov and E. N. Brodskaya, The Molecular Dynamics Simulation of a Small Drop, *Interface Sci.*, Vol. 62, pp. 542–555, 1977.
130. S. H. Park, J.-G. Weng, and C.-L. Tien, A Molecular Dynamics Study on Surface Tension of Microbubbles, *Int. J. Heat Mass Transfer*, Vol. 44, pp. 1849–1856, 2001.
131. R. C. Tolman, The Effect of Droplet Size on Surface Tension, *J. Chem. Phys.*, Vol. 17, pp. 333–337, 1949.
132. S. M. Thompson, K. E. Gubbins, J. P. R. B. Walton, R. A. R. Chantry, and J. S. Rowlinson, A Molecular Dynamics Study of Liquid Drops, *J. Chem. Phys.*, Vol. 81, pp. 530–542, 1984.
133. A. E. van Giessen and E. M. Blokhuis, Determination of Curvature Corrections to the Surface Tension of a Liquid-Vapor Interface through Molecular Dynamics Simulations, *J. Chem. Phys.*, Vol. 116, pp. 302–310, 2002.
134. K. Koga, X. C. Zeng, and A. K. Shchekin, Validity of Tolman's Equation: How Large Should a Droplet Be?, *J. Chem. Phys.*, Vol. 109, pp. 4063–4070, 1998.
135. T. V. Bykov and X. C. Zeng, A Patching Model for Surface Tension and the Tolman Length, *J. Chem. Phys.*, Vol. 111, pp. 3705–3713, 1999.
136. J. Koplik and J. R. Banavar, Molecular Dynamics of Interface Rupture, *Phys. Fluids A*, Vol. 5, pp. 521, 1993.
137. S. Kawano, Molecular Dynamics of Rupture Phenomena in a Liquid Thread, *Phys. Rev. E*, Vol. 58, pp. 4468, 1998.
138. M. Moseler and U. Landman, Formation, Stability, and Breakup of Nanojets, *Science*, Vol. 289, pp. 1165–1169, 2000.
139. P. K. Schelling, S. R. Phillpot, and P. Keblinski, Phonon Wave-Packet Dynamics at Semiconductor Interfaces by Molecular-Dynamics Simulation, *Appl. Phys. Lett.*, Vol. 80, pp. 2484–2486, 2002.